

# Synthesis and Biological Evaluation of Dihydropyrano-[2,3-c] Pyrazole as a New Class of PPAR $\gamma$ Partial Agonists

Mr. Ramesh Bhalchandra Dongare

Lecturer selection grade, Bharati Vidyapeeth Institute of Technology, Navi Mumbai, India

**ABSTRACT:** Peroxisome proliferator-activated receptor  $\gamma$  (PPAR $\gamma$ ) is a well-known target for thiazolidinedione antidiabetic drugs. In this paper, we present the synthesis and biological evaluation of a series of dihydropyrano [2, 3-c] pyrazole derivatives as a novel family of PPAR $\gamma$  partial agonists. Two analogues were found to display high affinity for PPAR $\gamma$  with potencies in the micro molar range. Both of these hits were selective against PPAR $\gamma$ , since no activity was measured when tested against PPAR $\alpha$ , PPAR $\delta$  and RXR $\alpha$ . In addition, a novel modeling approach based on multiple individual flexible alignments was developed for the identification of ligand binding interactions in PPAR $\gamma$ . In combination with cell-based transactivation experiments, the flexible alignment model provides an excellent analytical tool to evaluate and visualize the effect of ligand chemical structure with respect to receptor binding mode and biological activity.

## I. INTRODUCTION

Peroxisome proliferator-activated receptors (PPARs) are ligand-activated transcription factors of the nuclear hormone receptor superfamily. Many cellular and systemic roles have been attributed to these receptors, reaching far beyond the stimulation of peroxisome proliferation in rodents after which they were initially named. The three PPAR subtypes PPAR $\alpha$ , PPAR $\delta$  and PPAR $\gamma$  exhibit broad, subtype-specific tissue expression patterns. The PPAR $\gamma$  subtype is most highly expressed in adipose tissue, and agonists for this receptor, increase adipocyte differentiation, enhance insulin sensitivity and improve lipid profiles. A variety of synthetic agonists for PPAR $\gamma$  have been studied in the area of antidiabetic drug discovery such as the full agonists thiazolidinedione's (TZDs), including rosiglitazone (**1**) and pioglitazone (**2**). These drugs are now well established in clinical practice for the treatment of type II diabetes. However, despite their effectiveness in lowering blood glucose levels and improving insulin sensitivity, they have recently been associated with severe side effects, such as fluid retention, weight gain, cardiac hypertrophy, and hepatotoxicity. Strong evidence suggest that these side-effects may be associated with full agonism, and much recent focus has been given to the development of partial agonists, which are expected to retain full insulin sensitizing effects with minimal side-effects. One such partial agonist, balaglitazone (**3**), was shown to activate PPAR $\gamma$  and improve glucose levels without causing undesirable accumulation of fluid and fat.

# International Journal of Innovative Research in Science, Engineering and Technology

(A High Impact Factor, Monthly, Peer Reviewed Journal)

Visit: [www.ijirset.com](http://www.ijirset.com)

Vol. 9, Issue 2, February 2020

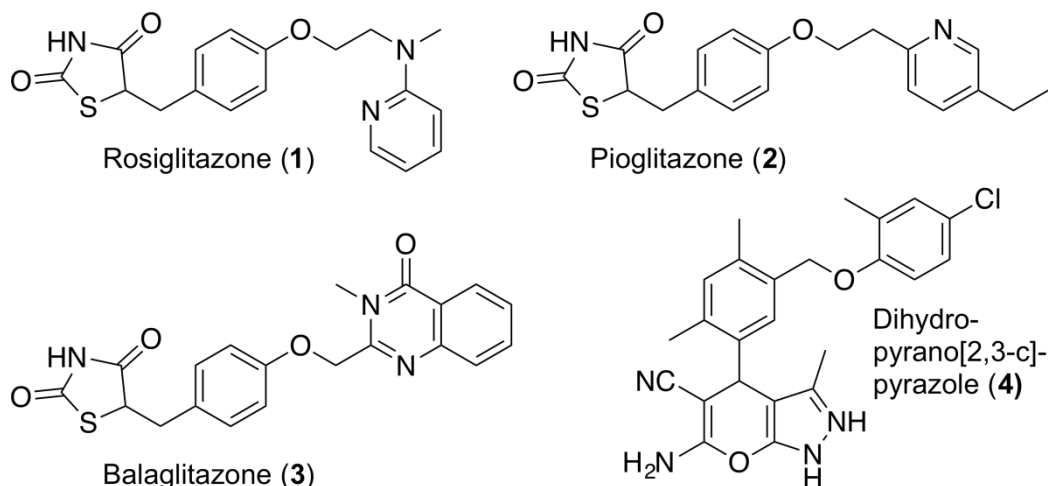


Figure1. Pharmacologically relevant PPAR $\gamma$  ligands.

In view of these developments, the discovery of novel selective PPAR $\gamma$  agonists with partial binding properties would be advantageous not only as candidates for the treatment of type II diabetes, but also as chemical probes to investigate the function of PPAR $\gamma$ , as new roles for it are currently being identified, e.g. as anti-obesity drug target.

Recently, we reported an integrated *in silico* / *in vitro* workflow, based on pharmacophore- and structure-based virtual screening of the ZINC library, coupled with competitive binding and transactivation assays, and adipocyte differentiation and gene expression studies. In this study, dihydropyrano [2,3-*c*]pyrazole **4** was identified as a promising PPAR $\gamma$  partial agonist combining high inhibitor activity ( $IC_{50} = 0.03$  mM) with a relatively poor induction of adipocyte differentiation. This promoted us to further investigate the dihydropyrano [2,3-*c*]pyrazoles as a novel class of PPAR $\gamma$  ligands. Herein, we present the development of a synthetically tractable scale-up synthesis of dihydropyrano[2,3-*c*]pyrazole **4** for further biological studies. Furthermore, we describe the synthesis and biological evaluation of a series of novel dihydropyrano [2,3-*c*]pyrazole derivatives with high structural variation.

## II. RESULTS AND DISCUSSION

### 2. Chemistry

#### 2.1 Dihydropyrano [2,3-*c*]pyrazoles.

Dihydropyrano [2,3-*c*]pyrazole constitute an important class of compounds with a wide range of biological properties, such as anticancer, antimicrobial and anti-inflammatory activities. Only recently, we published data that identified the dihydropyrano [2,3-*c*]pyrazole **4** as a promising PPAR $\gamma$  partial agonist for the treatment of type II diabetes.

The most common and convenient approach towards diverse dihydropyrano[2,3-*c*]pyrazoles is a two-step procedure comprising the following steps: (1) Condensation of hydrazine derivative **5** is condensed with  $\beta$ -keto ester **6** under basic conditions to produce the 1*H*-pyrazol-5(4*H*)-one derivative **7**; (2) Three-component base-catalyzed reaction of 1*H*-pyrazol-5(4*H*)-one **7**, aromatic aldehyde **8** and malononitrile **9**. The three-component reaction involve a tandem Michael addition-Thorpe-Ziegler-type reaction, followed by tautomerization to generate the dihydropyrano[2,3-

# International Journal of Innovative Research in Science, Engineering and Technology

(A High Impact Factor, Monthly, Peer Reviewed Journal)

Visit: [www.ijirset.com](http://www.ijirset.com)

Vol. 9, Issue 2, February 2020

c]pyrazole core **10**. It should be noted that these compounds may exist in the 1,4-dihydro or 2,4-dihydro tautomer forms when the N1 position is substituted ( $R^1 = H$ ).

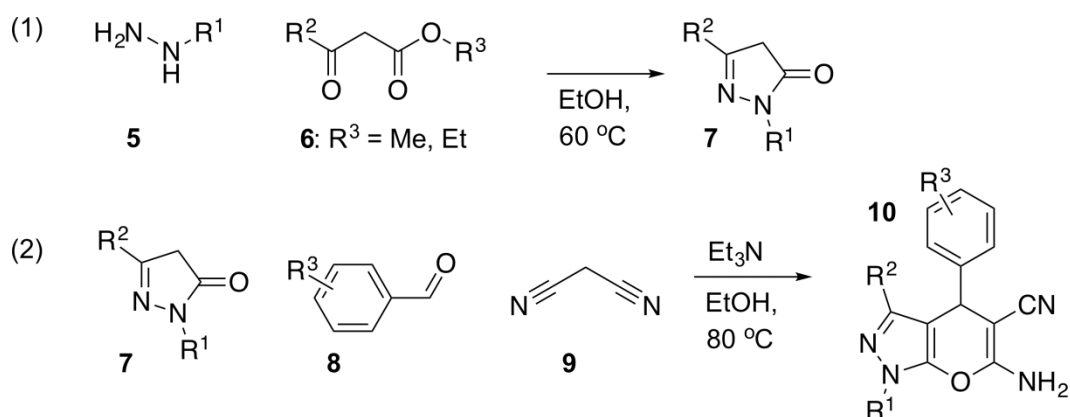


**Figure2.** Reaction pathway for the synthesis of dihydropyrano [2,3-c] pyrazole derivatives **10**.

The presented protocol represents a synthetically tractable strategy for drug discovery as the target molecule is synthesized in two high-yielding steps without the need for time-consuming chromatography. Furthermore, the general two-step sequence is easily amenable to the preparation of combinatorial libraries of diverse dihydropyrano[2,3-c]pyrazoles. Given the large number of commercially available aldehydes and the easy access to hydrazines and  $\beta$ -keto esters, this method provides access to dihydropyrano[2,3-c]pyrazole libraries with high appendage diversity introduced through substituents at the 1-, 3-, and 4-positions.

## 2.2 Scale-up synthesis of lead compound **4**.

Dihydropyrano[2,3-c]pyrazole **4** is a promising PPAR $\gamma$  partial agonist, that may serve as an entry for the development of new antidiabetics. We initiated our studies by developing a practical and gram-scale synthesis of **4** for compound validation, further medicinal chemistry evaluation, and lead optimization studies.

Considering the synthetic strategy outlined in, aldehyde building block **15** constitutes a key intermediate for the scale-up synthesis of **4**. The readily available bromomethylbenzaldehyde **14** was identified as the most readily available precursor to aldehyde **15**. Our stepwise synthesis of **14** commenced with *m*-xylene, which was bischloromethylated to afford 1,5-bis(chloromethyl)-2,4-dimethylbenzene **12**. This was then converted to dialdehyde **13** in a Sommelet reaction, following a procedure developed by Wood. Selective reduction of one of the aldehyde moieties with  $NaBH_4$  and subsequent treatment of the resulting monoalcohol with  $HBr$  in boiling  $AcOH$  afforded the bromomethylbenzaldehyde **14**. Compound **14** was quantitatively converted to aldehyde **15** by reaction with 4-chloro-2-methylphenol in acetonitrile at 50 °C in the presence of  $K_2CO_3$ .

With substantial amounts of key intermediate **15** in hand, we investigated the final tandem Michael addition-Thorpe-Ziegler reaction to generate the desired dihydropyrano [2,3-c] pyrazole. Reactant **17** was easily available from ethyl acetoacetate and hydrazine hydrate (90% yields after re-crystallization). Finally, treatment of **17** with aldehyde **14** and malononitrile in EtOH resulted in precipitation of **4** directly from the reaction mixture as a pure, white powder in 72% yield.

## International Journal of Innovative Research in Science, Engineering and Technology

(A High Impact Factor, Monthly, Peer Reviewed Journal)

Visit: [www.ijirset.com](http://www.ijirset.com)

Vol. 9, Issue 2, February 2020

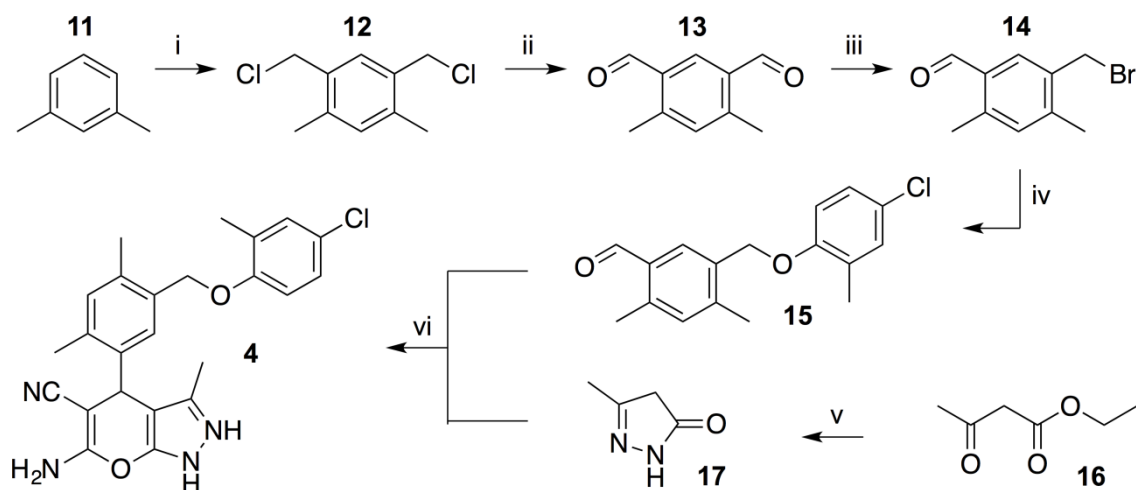


Figure 3. Reaction pathway for the synthesis of dihydropyrano [2,3-*c*]pyrazole 4.

### 2.3 Synthesis of 1,4-dihydropyrano-[2,3-*c*]pyrazoles.

Next, the two-step protocol was applied to prepare a collection of 1,4-dihydropyrano[2,3-*c*]pyrazoles. All starting hydrazines were purchased from commercial suppliers. The corresponding  $\beta$ -keto esters were synthesized either according to Yuasa and Tsurutaor by deprotonation of esters and subsequent reaction with ethyl acetate. Aldehydes were all purchased or prepared in one step from **14** according to the procedure described for the synthesis of **15**. Following the general procedure, a library of 32 structurally diverse 1,4-dihydropyrano[2,3-*c*]pyrazoles were synthesized. The ease of this procedure should be emphasized. The reaction was performed at 80°C for 2 h and upon cooling to room temperature, nearly all products precipitated as discrete powders with no need for further purification.

# International Journal of Innovative Research in Science, Engineering and Technology

(A High Impact Factor, Monthly, Peer Reviewed Journal)

Visit: [www.ijirset.com](http://www.ijirset.com)

Vol. 9, Issue 2, February 2020

Entry	Substrate	Yield	hPPAR $\gamma$ LBD transactivation	hPPAR $\gamma$ LBD ligand displacement IC <sub>50</sub> ( $\mu$ M)	Entry	Substrate	Yield	hPPAR $\gamma$ LBD transactivation	hPPAR $\gamma$ LBD ligand displacement IC <sub>50</sub> ( $\mu$ M)
1		72%	+ <sup>c</sup>	32	18		58%	- <sup>a</sup>	-
2		57%	+ <sup>c</sup>	46	19		88%	- <sup>a</sup>	-
3		63%	- <sup>a</sup>	15.7	20		80%	+ <sup>c</sup>	14
4		12%	+ <sup>c</sup>	104	21		71%	- <sup>a</sup>	28
5		77%	- <sup>a</sup>	84	22		75%	- <sup>aa</sup>	-
6		78%	- <sup>a</sup>	-	23		79%	- <sup>a</sup>	-
7		39%	- <sup>a</sup>	3.0	24		8%	+ <sup>c</sup>	59
8		94%	+ <sup>c</sup>	105	25		58%	- <sup>a</sup>	87
9		89%	- <sup>a</sup>	173	26		84%	- <sup>a</sup>	-
10		89%	- <sup>a</sup>	75	27		84%	+ <sup>c</sup>	407
11		77%	- <sup>a</sup>	-	28		54%	+ <sup>c</sup>	-
12		58%	- <sup>a</sup>	-	29		56%	- <sup>a</sup>	-
13		88%	- <sup>a</sup>	-	30		15%	+ <sup>c</sup>	215
14		80%	+ <sup>c</sup>	14	31		7%	+ <sup>c</sup>	0.52
15		48%	- <sup>a</sup>	31	32		3%	+ <sup>c</sup>	1.1
16		50%	- <sup>a</sup>	-	33		8%	- <sup>a</sup>	14
17		50%	+ <sup>c</sup>	91					

<sup>a</sup>Synthesized according to Scheme 1. <sup>b</sup>Synthesized according to Figure 2. <sup>c</sup>Activation (more than 2-fold). <sup>d</sup>No activation (less than 2-fold).

**Figure4. Chemical and biological data for dihydropyrano [2, 3-c] pyrazole.**

## 2.4 Biological evaluation

### 2.4.1 Competitive binding and transactivation assays.

The dihydropyrano[2,3-c]pyrazoles 4, 10a-10ag were tested for transactivation and affinity from competitive binding assay. Twenty-three of the dihydropyrano[2,3-c]pyrazoles dose-dependently displaced a labeled PPAR $\gamma$  ligand *in vitro* in a TR-FRET competitive binding assay. Potency of binding as compared with known PPAR ligands was ranging from low affinity, as for compound 10c, 10g, 10h, 10aa and 10ad with IC<sub>50</sub> > 100  $\mu$ M, to fairly high affinity, as observed for compound 10ae and 10af (IC<sub>50</sub>  $\leq$  1  $\mu$ M). Rosiglitazone was measured to displace with an IC<sub>50</sub> of 58 nM in this assay, in agreement with previously reported affinities. Further, to examine receptor binding at a more functional level, we analyzed the ability of the compounds to induce transcriptional activation in a cell based transactivation assay. Fourteen compounds were found to stimulate PPAR $\gamma$ -mediated transactivation. As several relatively potent binders

# International Journal of Innovative Research in Science, Engineering and Technology

(A High Impact Factor, Monthly, Peer Reviewed Journal)

Visit: [www.ijirset.com](http://www.ijirset.com)

Vol. 9, Issue 2, February 2020

(compounds 10b, 10f and 10ag) did not induce transcriptional activation, we speculated whether these compounds were behaving as antagonists. However, both cellular uptake and compound “metabolism” could influence the actual concentration, and it cannot be excluded that some of the compounds did not reach saturating concentrations in the cell-based transactivation assay.

It was indeed observed that most of the tested dihydropyrano[2,3-*c*]pyrazole compounds showed some activity against the PPAR $\gamma$  receptor, with the exception of compounds 10e, 10j, 10k, 10l, 10z, 10ab and 10ac. In analogy with previous SAR analyses of PPAR $\gamma$  interacting compound series, the resulting SAR is not easily interpreted. However, it appears that the 2, 5-dimethylaryl (10a, 10g, 10p, 10ab, 10ae) and the N1 4-Cl-phenyl moieties (**10ae**, **10af**) are structural elements that confer transactivation to the dihydropyranoazole scaffold. Furthermore, a strong correlation was observed between structure and binding affinity for the compounds, with the two N1 4-chlorophenyl-substituted dihydropyrano [2,3-*c*]pyrazoles (10ae and 10af) both being identified as high-affinity binders with potency in the micro molar range.

The two most potent hits (10ae and 10af) were further tested for transactivation selectivity towards all three PPAR subtypes. Both of the hits were found to be selective against PPAR $\gamma$ .

## 2.4.2 Evaluation of PPAR $\gamma$ binding mode.

The binding modes of the dihydropyrano [2,3-*c*]pyrazoles **4**, **10a-10ag** were explored with the multiple individual alignment approach. For this purpose, a model set of PPAR $\gamma$  template ligands was generated on the basis of PPAR $\gamma$  agonist-receptor complexes from the Protein Data Bank (PDB). More specifically, the template set was created from twenty-three PDB PPAR $\gamma$  ligands accounting eleven full and twelve partial agonists. Each template was made from an agonist-bound PPAR $\gamma$  structure and removal of the receptor leaving the template agonist in its crystal conformation. Afterwards, individual alignment attempts of a given test molecule on each of the generated templates followed by reintroduction of the receptor and energy calculation, provided a hit list of matching binding modes. According to the targets encoded by these templates, a binding profile for the test ligand was generated.

In order to identify and implement rational threshold values for the docking screen, all twenty-three known PPAR $\gamma$  model ligands were docked with the procedure described above. It was found that all model-ligands could be identified by their own template. To prioritize the best hits and reduce the number of false positives, the internal strain ( $dU$ ), configurationally similarity ( $dF$ ) and alignment score ( $dS$ ) constraints were set to a threshold value of 1. Furthermore, only compounds with an Auto dock docking score ( $\Delta G$ ) more negative than a threshold value of -10 kcal/mol passed the docking screen, while any remaining compounds were discarded.

To validate the model, a test set of twenty-four known PPAR $\gamma$  ligands, including nine full agonists, seven partial agonists, and eight inactives, was collected from the literature. The set of agonists was constituted by known antidiabetic drugs, including rosiglitazone (**1**, TZD), farglitazar (non-TZD) and other biological relevant agonist with either selective PPAR $\gamma$  or dual PPAR $\alpha/\gamma$ , PPAR $\delta/\gamma$  selectivity, but no pan PPAR agonists were included. It was ensured that the compounds covered a broad range of activities, from weak to medium and strong agonists. The inactives were manually selected from a set of PPAR $\gamma$  inactive compounds that were structurally similar to the selected PPAR $\gamma$  agonists. Upon evaluation of the test set of PPAR $\gamma$  ligands in the model, seven of the nine full agonists were found to match a full agonist template (with the exception of CID-11384748 and CID-44411945) with four of them matching on more than one template. Six out of seven partial agonists were observed to align on a partial agonist template (with the exception of CID-15069295). Unfortunately, due to the high structural similarity between actives and inactive, the model was not always able to discriminate between the two, leading to several of the inactive test compounds being identified as actives (false positives). However, in combination with cell-based transactivation experiments, the presented model provides a promising analytical tool to evaluate and visualize the effect of ligand chemical structure in respect to receptor binding mode and biological activity.

## International Journal of Innovative Research in Science, Engineering and Technology

(A High Impact Factor, Monthly, Peer Reviewed Journal)

Visit: [www.ijirset.com](http://www.ijirset.com)

Vol. 9, Issue 2, February 2020

Next, the methodology was applied to the reference dihydropyrano[2,3-c]pyrazole PPAR $\gamma$  partial agonist **4**. The ligand **4** was found to match two of the partial agonist templates (CID-2742752 and CID-10229498). From further inspection of the suggested binding modes, it was concluded that the CID-10229498 binding mode is reasonable. The dihydropyrano[2,3-c]pyrazole group of **4** was observed to make several stabilizing hydrophobic interactions in the  $\beta$ -sheet regions, while the amino group formed a hydrogen bond with Ile281 located in Helix3. Furthermore, the central benzene ring made strong interactions with Cys285.

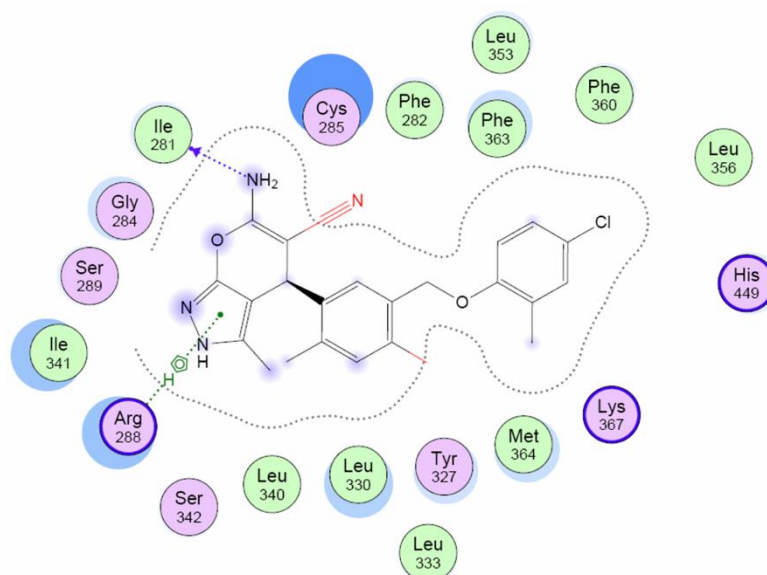


**Figure5. The ligand 4 presented in the aligned binding mode on CID-10229498.**

Finally, we analyzed the binding modes of 32 novel potential PPAR $\gamma$  partial agonists (**10a-10ag**) by incorporation in twenty-three ligand templates in the individual alignment model. Of the 32 compounds analysed by the model, we were able to identify binding modes for twenty-one of them. All ligands without identifiable binding modes were found to be low affinity binders ( $IC_{50} < 30$  mM) in the ligand displacement experiments.

Six of the dihydropyrano [2,3-c]pyrazole compounds (**10q, 10r, 10s, 10ae, 10af and 10ag**) displaying highest transactivation potential were found to match the same CID-10229498 template as reference dihydropyrano[2,3-c]pyrazole **4**. A closer inspection of the docked ligands revealed that although all of the six ligands matched the same template, they clustered around two distinct binding modes. A strong correlation between binding mode and chemical structure was observed. The ligands **10q, 10r** and **10s** share high structural similarity with dihydropyrano [2,3-c]pyrazole **4** and were all observed to have identical alignments in the CID-10229498 template displaying the same types of interactions as described for **4**. However, the presence of a substituent on the dihydropyrano[2,3-c]pyrazole N1 clearly influences the receptor ligand complex. The high-affinity ligands **10ae, 10af** and **10ag** have a N1 phenyl-substituent in common. Although they were recognized to match the CID-10229498 template, they seemed to adopt a different but mutually similar scaffold positioning. The altered ligand structure induces a relocation of the ligand in the receptor, allowing the dihydropyrano[2,3-c]pyrazole phenyl-group to participate in several stabilizing hydrophobic interactions with Ser342 and Ile341 in the  $\beta$ -sheet regions. The altered positioning places the pyrano[2,3-c]pyrazole moiety in close proximity to Helix3, where strong interactions with Cys285 are observed. Furthermore, the carbonitrile group may interact with Arg288.

# International Journal of Innovative Research in Science, Engineering and Technology

(A High Impact Factor, Monthly, Peer Reviewed Journal)

Visit: [www.ijirset.com](http://www.ijirset.com)

Vol. 9, Issue 2, February 2020

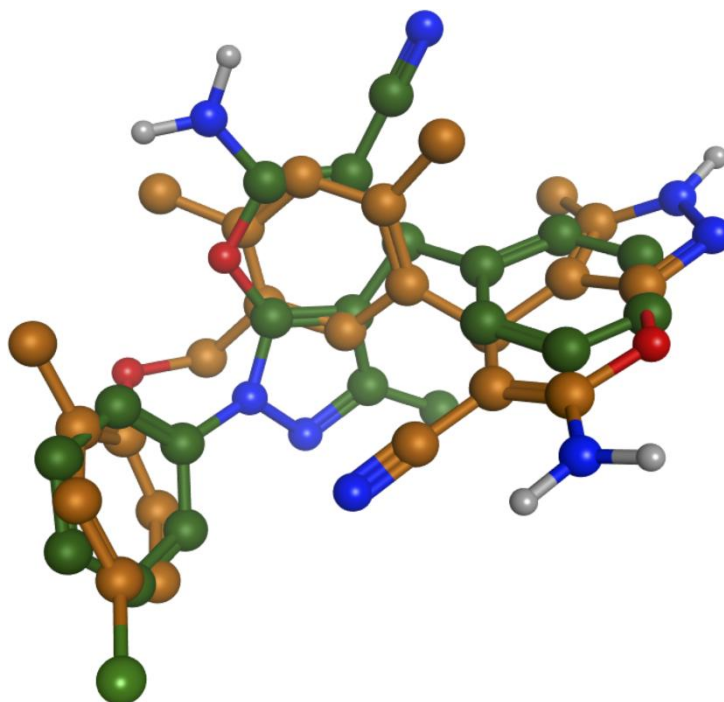


Figure6. The ligands 4 (orange) and 10ag (green) shown on top of each other from alignment on CID-10229498.

## III. EXPERIMENTAL SECTION

### 3.1 Materials and measurements

All reagents used were commercially available. All solvents were of HPLC grade. Analytical LC-MS analysis was performed on a Waters AQUITY UPLC system equipped with PDA and SQD MS detector; column: AQUITY UPLC BEH C18 1.7 $\mu$ m, 2.1 x 50mm; column temp: 65°C; solvent A: 0.1% formic acid (aq); solvent B: 0.1% formic acid (acetonitrile); gradient: 5% B to 100% B in 2.4 min, hold for 0.1 min, total run-time ca. 2.6 min.  $^1\text{H}$  and  $^{13}\text{C}$  NMR 300 MHz spectra were recorded on a Varian Mercury 300 BB spectrometer at room temperature. All NMR spectra were recorded using  $\text{CDCl}_3$  or  $\text{DMSO-}d_6$  as solvents

### 3.2 Synthesis

#### 3.2.1 3-Bis (chloromethyl)-4, 6-dimethylbenzene (12).

A stirred solution of *m*-xylene (100.0 mL, 0.818 mol), paraformaldehyde (58.0 g, 1.93 mol), acetic acid (99%, 200 mL) and conc. HCl (aq, 800 mL) was mechanically stirred for 48 h at 70°C. During the last part of the reaction time (18 h), the product precipitated as a white solid. The reaction mixture was cooled to room temperature, and the product isolated by filtration. The filter cake was washed with water and then dissolved in boiling heptane (200 mL). The boiling heptane phase was washed with hot 10% aqueous  $\text{NaHCO}_3$  (50 mL) and then phase separated. Upon cooling to room temperature, the product precipitated as a white solid. Yield: 60.3 g (37%).  $^1\text{H}$  NMR (300 MHz,  $\text{CDCl}_3$ ):  $\delta$  = 7.26

# International Journal of Innovative Research in Science, Engineering and Technology

(A High Impact Factor, Monthly, Peer Reviewed Journal)

Visit: [www.ijirset.com](http://www.ijirset.com)

Vol. 9, Issue 2, February 2020

(s, 1H, ArH), 7.06 (s, 1H, ArH), 4.58 (s, 4H, CH<sub>2</sub>Cl), 2.40 (s, 6H, 2 × ArCH<sub>3</sub>); <sup>13</sup>C NMR (75 MHz, CDCl<sub>3</sub>): δ = 138.09, 133.61, 133.38, 131.33, 44.50, 18.54.

### 3.2.2, 6-Dimethylisophthalaldehydebenzene (13).

A stirred suspension of 1, 3-bis (chloromethyl)-4, 6-dimethylbenzene (**12**) (80.0 g, 0.394 mol), hexamethylenetetramine (110.5 g, 0.789 mol), ethanol (1000 mL) and water (500 mL) was refluxed for 16 h. The hot reaction mixture was filtered and the filtrate cooled to room temperature. The pH was adjusted to 1–2 with 4.0 M HCl (aq) and extracted with CH<sub>2</sub>Cl<sub>2</sub> (3 × 700 mL). The combined organic phase was dried with Na<sub>2</sub>SO<sub>4</sub>, filtered and solution concentrated to around 100 mL under reduced pressure. This resulted in precipitation of 4,6-dimethylisophthal-aldehydebenzene as a white solid, which was isolated by filtration. Yield: 23.3 g (37%). <sup>1</sup>H NMR (300 MHz, CDCl<sub>3</sub>): δ = 10.25 (d, J = 0.6 Hz, 2H, 2 × CHO), 8.22 (s, 1H, ArH), 7.18 (s, 1H, ArH), 2.70 (d, J = 0.9 Hz, 6H, 2 × ArCH<sub>3</sub>); <sup>13</sup>C NMR (75 MHz, CDCl<sub>3</sub>): δ = 191.71, 146.38, 136.94, 135.82, 132.78, 20.18; UPLC-MS (ESI): m/z = 163.1 (M+H)<sup>+</sup>.

### 3.2 3-Bromomethyl-2,4-dimethylbenzaldehyde (14).

4, 6-Dimethylisophthalaldehyde (23.3 g, 0.144 mol) was dissolved in EtOH (500 mL) with vigorous stirring at room temperature. The reaction mixture was then treated with NaBH<sub>4</sub> (0.55 g, 0.0146 mol) in one portion. After stirring for 2 h at room temperature, the solution was treated with another portion of NaBH<sub>4</sub> (0.55 g, 0.0146 mol). After additional 2 h of stirring, the reaction mixture was treated with a third portion of NaBH<sub>4</sub> (0.38 g, 0.010 mol) and the reaction mixture was left with stirring overnight at room temperature. EtOH was removed under reduced pressure and the remaining oil was treated with boiling water (200 mL) and the mixture cooled to room temperature. Acidification to pH 1–2 with 4.0 M HCl (aq) and treatment with brine (200 mL) and EtOAc (300 mL) afforded a two-phase system, which was separated. The water phase was extracted with EtOAc (2 × 200 mL). The combined organic phase was washed with brine (200 mL), dried over Na<sub>2</sub>SO<sub>4</sub>, filtered and concentrated *in vacuo*. The resulting yellow oil was purified by flash column chromatography on silica gel (eluent: heptane/EtOAc, 95:5) to afford 7.5 g (23%) of 5-bromomethyl-2,4-dimethyl-benzaldehyde (**14**) as a white solid and 6.0 g (26%) of recovered 4,6-dimethylisophthalaldehyde (**13**). <sup>1</sup>H NMR (300 MHz, CDCl<sub>3</sub>): δ = 10.20 (s, 1H, CHO), 7.74 (s, 1H, ArH), 7.10 (s, 1H, ArH), 4.53 (s, 2H, CH<sub>2</sub>Br), 2.63 (s, 3H, ArCH<sub>3</sub>), 2.45 (s, 3H, ArCH<sub>3</sub>); <sup>13</sup>C NMR (75 MHz, CDCl<sub>3</sub>): δ = 191.82, 143.80, 141.37, 134.54, 134.21, 133.46, 132.64, 31.20, 19.27, 19.13; UPLC-MS (ESI): m/z = 227.1, 229.1 (M+H)<sup>+</sup>.

### 3.2 4-((4-Chloro-2-methylphenoxy)methyl)-2,4-dimethylbenz-aldehyde (15).

5-Bromomethyl-2,4-dimethylbenzaldehyde (1.0 g, 4.40 mmol) and 4-chloro-2-methylphenol (657 mg, 4.62 mmol) were dissolved in acetonitrile (50 mL) and treated with K<sub>2</sub>CO<sub>3</sub> (912 mg, 6.60 mmol). The suspension was heated to 50°C with stirring. After 3 h the precipitate was removed by filtration and the filtrate concentrated *in vacuo*. Purification by flash column chromatography on silica gel (eluent: heptane/EtOAc 95:5) to afford the aldehyde **15** as a white solid. Yield: 1.26 g (99%). <sup>1</sup>H NMR (300 MHz, CDCl<sub>3</sub>): δ = 10.22 (d, J = 0.9 Hz, 1H, CHO), 7.84 (s, 1H, ArH), 7.20–7.07 (m, 2H, ArH), 6.83 (dd, J = 8.0, 1.1 Hz, 1H, ArH), 5.02 (s, 2H, OCH<sub>2</sub>Ar) 2.65 (s, 3H, ArCH<sub>3</sub>), 2.40 (s, 3H, ArCH<sub>3</sub>), 2.22 (d, J = 0.8 Hz, 3H, ArCH<sub>3</sub>); <sup>13</sup>C NMR (75 MHz, CDCl<sub>3</sub>): δ = 192.29, 155.38, 143.27, 140.71, 134.17, 133.27, 132.31, 132.26, 130.71, 129.05, 126.49, 125.59, 112.35, 68.23, 19.31, 19.23, 16.38; UPLC-MS (ESI): m/z = 289.2 (M+H)<sup>+</sup>.

### 3.2 5-Methyl-1H-pyrazol-5(4H)-one (17) [18].

Ethyl acetoacetate (10.0 g, 0.077 mol) was dissolved in EtOH (150 mL) and cooled to 0°C. With stirring the solution was treated dropwise with hydrazine hydrate (3.5 g, 0.070 mol). After complete addition the solution was heated to

# International Journal of Innovative Research in Science, Engineering and Technology

(A High Impact Factor, Monthly, Peer Reviewed Journal)

Visit: [www.ijirset.com](http://www.ijirset.com)

Vol. 9, Issue 2, February 2020

60°C for 3 h and the concentrated *in vacuo*. The resulting solid was re-crystallized from Et<sub>2</sub>O/EtOAc/EtOH to give **17** as a light yellow powder. Yield: 6.2 g (90%). <sup>1</sup>H NMR (300 MHz, DMSO-*d*<sub>6</sub>): δ = 10.40 (bs, 2H, NH + OH (tautomericenol form)), 5.21 (s, 1H, CH = COH (tautomericenol form)), 2.08 (s, 3H, ArCH<sub>3</sub>); <sup>13</sup>C NMR (75 MHz, CDCl<sub>3</sub>): δ = 161.22, 139.54, 89.03 (tautomericenol form), 49.37 (tautomericetto form), 11.28.

### 3.3 Competitive binding assays

IC<sub>50</sub> values for respective compounds were determined by competitive binding using time-resolved fluorescence resonance energy transfer (LanthaScreen, Invitrogen) on a Victor2 micro plate reader (PerkinElmer). Briefly, a terbium labeled anti-GST antibody was used to label purified GST-tagged PPARγ-LBD (ligand binding domain). Energy transfer from terbium to the tracer, a fluorescent pan PPAR agonist, enabled read-out of each test compounds' ability to displace the tracer. RFU values from dose-response curves (triplicate sampling) for test compounds as well as positive controls (rosiglitazone) were then analyzed using GraphPad Prism. An unrestrained sigmoidal (one-binding site) dose-response curve was fitted to each data set by linear regression and allowing for determination of IC<sub>50</sub> values. All compounds were tested in 10 different concentrations ranging from 3 nM to 500 μM (rosiglitazone from 0.3 nM to 10 μM).

### 3.4 Nuclear receptor-LBD transactivation

Hepa 1–6 cells were grown in minimum essential medium (MEM) (Gibco) supplemented with 10% fetal calf serum (FCS) and antibiotics (62.5 μg/mL penicillin and 100 μg/mL streptomycin).

Mouse embryo fibroblasts (MEFs) were propagated in Dulbeccos Modified Eagle's Media (DMEM) supplemented with 10% FCS and antibiotics.

Cells (Hepa 1–6 were used for PPARα whereas MEFs were used for PPARγ, PPARδ and RXRα transfections) were transfected in solution by Metafectene (Biontix) lipofection, essentially according to the manufacturer's instructions and seeded in media (MEM or DMEM supplemented with 10% fetal calf serum and antibiotics in 96-well dishes at 24000 cells/cm<sup>2</sup>. The transfection plasmid mix included the Gal4-responsive luciferase reporter, the expression vector for the fusion between the Gal4 DNA-binding domain and the nuclear receptor ligand binding domains, and a CMV-Renilla luciferase normalization vector (pRL-CMV, Promega). Six hours after addition of transfection mix to the cells, the media was changed to media (MEM or DMEM) supplemented with vehicle (0.1% DMSO), positive control (1 μM Rosiglitazone, 30 nM GW7647, 1 μM L165041 or 0.2 μM LG1069 for PPARγ, PPARα, PPARδ and RXRα, respectively), or compound. Approx. 18 hours later, cells were harvested and lysates analyzed for Photinus and Renilla luciferase activity by luminometry. All data points were performed in at least triplicate and each sample measured in duplicate. Luminometer raw data was analyzed in Microsoft Excel spreadsheets and presented as column graphs depicting average values of triplicates and including standard deviations.

### 3.5 Multiple flexible alignment template

Evaluation of the dihydropyrano[2,3-*c*]pyrazoles **4**, **10a-10ah** PPARγ binding modes was carried out using a multiple flexible alignment approach. The model was developed, refined and evaluated using the flexible alignment application of the MOE software. The agonist model set was generated using the SVL Batch FlexAlign script, based on a PDB compound set of eleven PPARγ full agonists and twelve seven PPARγ partial agonists. The set of model agonists was composed of known antidiabetic drugs, including Rosiglitazone (TZD) and Farglitazar (non-TZD) and other biological relevant agonist with either selective PPARγ or dual PPAR-α/γ, PPAR-δ/γ selectivity; no pan PPAR agonists were included. The compound set employed in the development of the PPARγ agonist binding model is given in the

# International Journal of Innovative Research in Science, Engineering and Technology

(A High Impact Factor, Monthly, Peer Reviewed Journal)

Visit: [www.ijirset.com](http://www.ijirset.com)

Vol. 9, Issue 2, February 2020

Supporting Information. The binding model was then used for the virtual screening of the library of the dihydropyrano[2,3-*c*]pyrazoles (**4**, **10a-10ah**). To be a hit, the test ligand pose had to fit the defined threshold of the binding model ( $\Delta G_{\text{intr}} = \Delta G - \Delta G_{\text{torsions}}$ , i.e. the torsion scoring term was excluded) less negative than a threshold value of -10 kcal/mol passed the docking screen, and the remaining compounds were discarded.

## IV. CONCLUSIONS

In here we report dihydropyrano [2,3-*c*]pyrazoles as a novel class of PPAR $\gamma$  partial agonists. A synthetically tractable scale-up synthesis of lead compound dihydropyrano [2,3-*c*]pyrazole **4** has been developed for compound validation as well as further medicinal chemistry efforts. Furthermore, the synthesis and biological evaluation of a series of novel dihydropyrano [2,3-*c*]pyrazole derivatives with high structural variation has been accomplished. Competitive binding and transactivation assay experiments showed that most of the compounds displayed some activity against PPAR $\gamma$  with the two NI 4-chlorophenyl-substituted dihydropyrano [2, 3-*c*] pyrazole (**10ae** and **10af**) both being identified as selective high-affinity binders with potency in the micro molar range.

Moreover, a novel approach based on multiple individual flexible alignments for the identification of ligand binding interactions in PPAR $\gamma$  was developed. In combination with cell-based transactivation experiments, the flexible alignment model provides an excellent analytical tool to evaluate and visualize the effect of ligand chemical structure in respect to receptor binding mode and biological activity.

## REFERENCES

1. Willson TM, Brown PJ, Sternbach DD, Henke BR. The PPARs: from orphan receptors to drug discovery. *J. Med. Chem.* 2000; 43(4): 527–550. pmid:10691680
2. Larsen TM, Toubro S, Astrup A. PPARgamma agonists in the treatment of type II diabetes: is increased fatness commensurate with long-term efficacy? *International Journal of Obesity* 2003; 27: 147–161. pmid:12586994
3. Haslam E. *Shikimic Acid Metabolism and Metabolites*, John Wiley & Sons: New York, 1993.
4. Elte J, Blicklé J. Thiazolidinediones for the treatment of type 2 diabetes. *Eur. J. Intern. Med.* 2007, 18(1): 18–25. pmid:17223037
5. Guan Y, Hao C, Cha D, Rao R, Lu W, Kohan D, et al. Thiazolidinediones expand body fluid volume through PPAR gamma stimulation of ENaC-mediated renal salt absorption. *Nat. Med.* 2005; 11: 861–866. pmid:16007095
6. Pan H, Lin Y, Chen Y, Vance D, Leiter E. Adverse hepatic and cardiac responses to rosiglitazone in a new mouse model of type 2 diabetes: Relation to dysregulated phosphatidylcholine metabolism. *Vasc. Pharmacol.* 2006; 45(1): 65–71.
7. Henriksen K, Byrjalsen I, Qvist P, Beck-Nielsen H, Hansen G, Riis BJ, et al. Efficacy and safety of the PPAR $\gamma$  partial agonist balaglitazone compared with pioglitazone and placebo: a phase III, randomized, parallel-group study in patients with type 2 diabetes on stable insulin therapy. *Diabetes Metab. Res. Rev.* 2011; 27(4): 392–401. pmid:21328517
8. Hwang J, Lee M, Kim H, Sung M, Kim H, Kim M, et al. Antiobesity effect of ginsenoside Rg3 involves the AMPK and PPAR- $\gamma$  signal pathways. *Phytother Res* 2008; 23(2): 262–266.
9. Kouskoumvekaki I, Petersen RK, Fratev F, Taboureau O, Nielsen TE, Oprea TI, et al. Discovery of a Novel Selective PPAR $\gamma$  Ligand with Partial Agonist Binding Properties by Integrated in Silico/in Vitro Work Flow. *J. Chem. Inf. Model* 2013; 53(4): 923–937. Pmid:23432662
10. Wang JL, Liu D, Zhang ZJ, Shan S, Han X, Srinivasula SM, et al. Structure-based discovery of an organic compound that binds Bcl-2 protein and induces apoptosis of tumor cells. *Proc. Natl. Acad. Sci. U.S.A.* 2000; 97(13): 7124–7129. Pmid:10860979
11. El-Tamany ES, El-Shahed FA, Mohamed BH. Synthesis and biological activity of some pyrazole derivatives. *J. Serb. Chem. Soc.* 1999; 64(1): 9–18.
12. Zaki MEA, Soliman HA, Hiekal OA, Rashad AE. Pyrazolopyranopyrimidines as a Class of Anti-Inflammatory Agents. *Z. Naturforsch. C* 2006; 61c: 1–5
13. Sharanin YA, Sharanina LG, Puzanova VV. Nitrile cyclization reaction. VII. Synthesis of 6-amino-4-aryl-3-methyl-5-cyano-1H,4H-pyrazolo[3,4-*b*]pyrans. *Zh. Org. Khim.* 1983; 19(12): 2609–2615.
14. Gerish M, Krumper JR, Bergman RG, Don Tilley T. Rhodium(III) and Rhodium(II) Complexes of Novel Bis(oxazoline) Pincer Ligands. *Organometallics* 2003; 22(1): 47–58.
15. Wood JH, Tung CC, Perry MA, Gibson RE. The Sommelet Reaction in the Synthesis of Aromatic Dialdehydes<sup>1</sup>. *J. Am. Chem. Soc.* 1950; 72(7): 2992–2993.
16. Esser B, Bandyopadhyay A, Rominger F, Gleiter R. From Metacyclophanes to Cyclacenes: Synthesis and Properties of [6.8]<sub>3</sub>Cyclacene. *Chem. Eur. J.* 2009; 15(14): 3368–3379. pmid:19280613